Electron and hole transport in undoped $Bi_{0.96}Sb_{0.04}$ alloys

B. Lenoir, M. O. Selme, A. Demouge, and H. Scherrer
Laboratoire de Physique des Matériaux, UMR 7556, Ecole des Mines, Parc de Saurupt, 54042 Nancy, France

Yu. V. Ivanov
A.F. Ioffe Physical-Technical Institute, 194021, St. Petersburg, Russia

Yu. I. Ravich
St. Petersburg State Technical University, 195251, St. Petersburg, Russia

(Received 17 November 1997; revised manuscript received 2 February 1998)

The complete set of the 12 independent galvanomagnetic coefficients was measured in weak magnetic fields in undoped $Bi_{0.96}Sb_{0.04}$ alloys within the temperature range 77–300 K. The analysis of these coefficients together with the two components of thermopower was fulfilled by the least-squares method using Hall and magnetoresistance factors. These factors were calculated based on a model taking into account the peculiarities of the band structure and the scattering of electrons and holes by acoustic phonons, as well as interband (recombination) scattering. The temperature dependence of carrier mobilities and densities was estimated and compared with that of pure bismuth. The mobilities of T holes are lower than those of electrons, and the difference in the alloy is more pronounced than in pure bismuth. The deviation from unity of the Hall and magnetoresistance factors of L electrons is greater than in bismuth. This result is confirmed through direct analysis of the experimental data on the galvanomagnetic coefficients. [S0163-1829(98)04518-4]

I. INTRODUCTION

Great emphasis has been put over the last 30 years,[1–3] and more recently,[4,5] on the study of the transport properties of $Bi_{1-x}Sb_x$ single crystals. Semiconducting alloys ($0.07 \leqslant x \leqslant 0.22$) were reported as presenting the best n-type thermoelectric performances around liquid nitrogen temperature,[2,3] whereas semimetallic alloys ($0 < x < 0.07$) have been found to be very attractive materials in thermomagnetic applications.[3]

Numerous studies performed on bismuth single crystals[6–12] showed that the analysis of the 12 measured independent galvanomagnetic coefficients in a weak magnetic field is a powerful method for the determination of carrier mobilities and densities. The least-squares procedure has been used in this analysis. However, the full set of the galvanomagnetic coefficients has not been measured in $Bi_{1-x}Sb_x$ alloys at any x until now.

The $Bi_{0.96}Sb_{0.04}$ alloy is interesting since the inversion of the two minima at the L point of the Brillouin zone at zero temperature leads to a transition to a gapless state; i.e., the direct energy gap becomes equal to zero. At higher temperatures, this energy gap increases,[13] as in pure bismuth,[14] and the arrangement of energy bands remains qualitatively similar to that of bismuth.

It has been shown, as a result of the calculation of galvanomagnetic coefficients in bismuth,[11,12,15] that the Hall and magnetoresistance factors of electrons governed by the energy dependence of the relaxation time differed significantly from unity at temperatures above 100 K, because of the strong nonparabolicity of the conduction band. These deviations of the factors from 1 lead to a significant change in the values of the carrier mobilities and densities. The analysis of five galvanomagnetic coefficients in the $Bi_{0.96}Sb_{0.04}$ alloy, performed by Demouge *et al.*,[16] showed that the difference from unity was greater in this alloy than in pure bismuth. It turned out that the difference of Hall and magnetoresistance factors from unity changed qualitatively the expressions of some galvanomagnetic coefficients.

Unfortunately, it is impossible to determine these two factors as fitted parameters by the least-squares procedure with sufficient accuracy. They must be calculated using a model of electron scattering. The results of these calculations can be compared to experimental results using simplified formulas for some magnetoresistance coefficients.[12] Another conclusion of the work by Demouge *et al.*[16] was that the hole contribution to the galvanomagnetic coefficients was lower in the alloy than in pure bismuth. Consequently, the accuracy of a hole mobility estimation from galvanomagnetic coefficients is low. Including two components of the thermopower into the set of the analyzed transport coefficients was suggested in the study of pure bismuth by the least-squares procedure[12] in order to improve the accuracy of both electron and hole mobilities. It is even more necessary in the study of the $Bi_{0.96}Sb_{0.04}$ alloy.

In the present work, the full set of the 12 independent galvanomagnetic coefficients in low magnetic fields was first experimentally determined in $Bi_{0.96}Sb_{0.04}$ alloys at temperatures ranging from 77 to 300 K. The analysis of these coefficients together with the two components of thermopower was then conducted by the least-squares procedure using Hall and magnetoresistance factors calculated from a model taking into account the strong nonparabolicity of the conduction band and a complex carrier-scattering mechanism. The temperature dependence of carrier mobilities and densities was estimated and compared with that of pure bismuth. Additionally, we present a direct proof that the Hall and mag-

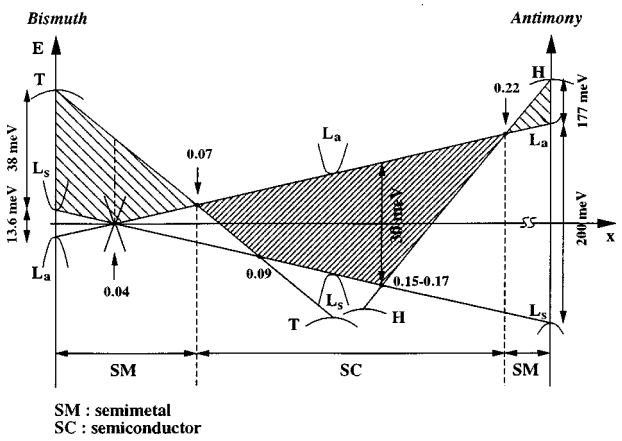

FIG. 1. Schematic representation of the energy bands near the Fermi level for $Bi_{1-x}Sb_x$ alloys as a function of x at $T=0$ K. For simplicity, the L-, T-, and H-point bands are drawn one on top of the others.

netoresistance factors of electrons deviate from unity in our analysis of the experimental data.

II. THEORY

A. Band model and initial parameters

$Bi_{1-x}Sb_x$ alloys form substitutional solid solutions over the whole range of concentration x. As x increases, the band structure of these alloys continuously transforms from the band structure of bismuth to the band structure of antimony (Fig. 1). The semimetallic properties of $Bi_{1-x}Sb_x$ in the interval $0 \leqslant x \leqslant 0.07$ are connected with a slight overlap of the three electron bands extrema at the L points of the Brillouin zone with a hole band extremum at the T point. At $x=0.04$,[17,18] the electron and hole bands at the L point cross in energy, leading to the appearance of a gapless state. The magnitude of the overlap between L and T bands decreases with increasing x, and for $0.07<x<0.22$, alloys are semiconductors with a small direct or indirect gap. For $x \geqslant 0.22$, the L extrema overlap with a new hole band located at the H point.

The electron Fermi surfaces in Bi-rich BiSb alloys correspond to three quasiellipsoids strongly elongated along direction tilted by an angle θ out of the binary-bisectrix plane [$\theta=6°$ in Bi (Ref. 19)]. The same structure occurs for the ''light'' L-hole band, which is separated from the electron band by a narrow energy gap E_g and which is coupled to the conduction band by the $\mathbf{k}\cdot\mathbf{p}$ interaction, resulting in a highly nonparabolic dispersion relation.

The simplest dispersion relation for the L bands is the two-band model of Lax and Mavroides.[20] Expressed in coordinates fixed to the ellipsoid axes, referred to as $(1',2',3')$, the energy dispersion law has the form

$$E\left(1+\frac{E}{E_g}\right)=\frac{\hbar^2}{2m_0}\,\mathbf{k}\cdot\begin{pmatrix} m_{1'L} & 0 & 0 \\ 0 & m_{2'L} & 0 \\ 0 & 0 & m_{3'L} \end{pmatrix}^{-1}\cdot\mathbf{k}, \quad (1)$$

where E is the electron energy measured from the bottom of the conduction band, m_0 the free electron mass, $m_{i'L}$ the effective masses at the edge of the bands, and $\mathbf{k}$ the wave vector.

TABLE I. Experimental values of E_g and $K(T,x=0.04)$ vs temperature according to Mendez's (Ref. 13) data.

T (K)	E_g (meV)	$K(T,x=0.04)$
78	1	1.12
100	2	1.16
120	3	1.20
140	5	1.23
180	8	1.34
220	12	1.52
300	23	2.20

The deviation of the T-hole band from parabolicity is much less than that of the L band and can be described satisfactorily by the following equation:

$$E=\frac{\hbar^2}{2m_0}\left[\frac{(k_1^2+k_2^2)}{M_{1T}}\right)+\frac{k_3^2}{M_{3T}}\Bigg], \quad (2)$$

where the subscripts 1, 2, and 3 refer to the binary, bisectrix, and trigonal directions, respectively. The energy E is measured from the top of the valence band, and $M_{1T}=M_{2T}$, M_{3T} are the effective masses.

Both the large nonparabolicity of the energy dispersion law for the conduction band and the strong dependence of the gap and electron effective masses on temperature,[13,14] pressure,[21,22] and composition[13] appear in Bi-rich BiSb alloys as consequences of the narrow gap at the L point.

The simple two-band model was applied for the description of the nonparabolicity in the study of the galvanomagnetic effects in bismuth[11,12,15] and in the $Bi_{0.96}Sb_{0.04}$ alloy.[16] This approach is adequate for the two $1'$ and $3'$ directions, but not for the $2'$ direction since the mass component $m_{2'L}$ is much larger than the two other components $m_{1'L}$ and $m_{3'L}$. Nevertheless, we applied the two-band model as the simplest approximation for all three directions, assuming that the error may be small in the final results of the calculations.

The temperature and composition dependences of the energy gap and the cyclotron effective masses of electrons for $Bi_{1-x}Sb_x$ alloys ($x<0.2$) have been studied by Mendez[13] using the magneto-optical method. The experimental results were close to the approximation where the effect of temperature T and composition x on the gap, $\Delta E_g(T)$ and $\Delta E_g(x)$, respectively, were considered as independent from each other. Taking into account that $E_g=0$ at $T=0$ K for the $Bi_{0.96}Sb_{0.04}$ alloy, we may apply the known magnitude $\Delta E_g(T)$ in pure Bi (Ref. 14) as being the full gap $E_g(T)$ for the alloy. The results are reported in Table I.

The magneto-optical experiments[13] gave also information about the light binary cyclotron effective mass of electrons, m_{cL}. This mass depends on the components $m_{1'L}$ and $m_{3'L}$ at the bottom of the conduction band as

$$m_{cL}\propto(m_{1'L}m_{3'L})^{1/2}. \quad (3)$$

In the two-band model, $m_{1'L}$ and $m_{3'L}$ must be proportional to the energy gap. According to experimental results,[13] the ratio m_{cL}/E_g increases slightly with a rise in T and x, giving a correcting coefficient $K(T,x)$ to the relation of proportionality of m_{cL} versus E_g. By interpolating Mendez's data, we obtained the coefficient $K(T,x)$ as a function of temperature for $x=0.04$ (Table I). These were used for the determination of the initial effective masses $m_{i'L}$ necessary for continuing our calculations, by applying the following formula:

$$m_{i'L}(T,x)=K(T,x)m_{i'L}(77,0)\,\frac{E_g(T,x)}{E_g(77,0)}, \tag{4}$$

with $E_g(77,0)=15.2$ meV, $m_{1'L}(77,0)=0.001\,53$, $m_{2'L}(77,0)=0.25$, and $m_{3'L}(77,0)=0.002\,81$ as determined in bismuth.[12,14]

Using the two-band model, we have to assume that the large effective mass $m_{2'L}$ depends on parameters x and T like the two small components $m_{1'L}$ and $m_{3'L}$. Accepting the more real constant value $m_{2'L}$ for the bottom of the conduction band, we should obtain a quite unreally large effective mass $m_{2'L}$ at energies near the chemical potential. The application of an unreally small effective mass $m_{2'L}$ proportional to very narrow gap E_g at the bottom leads on the contrary to a reasonable value near the chemical potential. Given that the final results depend weakly on the large component of the effective mass, a correct order of magnitude of this component is sufficient to achieve satisfactory calculations.

The T-hole effective masses have been previously calculated versus temperature in pure bismuth.[11] It was shown that these values are weakly temperature dependent. Since no information is available on alloys, we used data for Bi obtained at low temperature:[23] $M_{1T}=0.0638$ and $M_{3T}=0.702$. We also assumed that they do not vary with temperature.

B. Galvanomagnetic and thermopower tensors

The phenomenological theory of low-field galvanomagnetic effects assumes Ohm's law to hold for the resistivity tensor $\bar{\bar{\rho}}(\mathbf{B})$ or its reciprocal, the conductivity tensor $\bar{\bar{\sigma}}(\mathbf{B})$ in the presence of a magnetic field $\mathbf{B}$:

$$\mathbf{E}=\bar{\bar{\rho}}(\mathbf{B})\mathbf{J} \quad \text{or} \quad \mathbf{J}=\bar{\bar{\sigma}}(\mathbf{B})\mathbf{E}, \tag{5}$$

where $\mathbf{E}$ is the electric field and $\mathbf{J}$ the current density. The theory assumes that $\bar{\bar{\rho}}(\mathbf{B})$ may be expanded in a power series of $\mathbf{B}$, if $\mathbf{B}$ is low enough. Retaining only terms to the second order, each component of the tensor may be written as follows:

$$\rho_{ij}(\mathbf{B})=\rho_{ij}+R_{ijk}B_k+A_{ijkl}B_kB_l. \tag{6}$$

Of course, the same development applies also for the conductivity tensor $\bar{\bar{\sigma}}(\mathbf{B})$.

The number of independent coefficients appearing in Eq. (6) is limited to 12 for $Bi_{1-x}Sb_x$ alloys belonging to the point group $R\bar{3}m$: two resistivities ρ_{11} and ρ_{33}, two Hall coefficients R_{123} and R_{231}, and eight magnetoresistance coefficients A_{11}, A_{33}, A_{14}, A_{41}, A_{12}, A_{13}, A_{31}, and A_{44}.

By determining voltages for a given set of $\mathbf{J}$ and $\mathbf{B}$, these 12 coefficients can be measured experimentally. For the purpose of comparing these experimental values with the calculations of the galvanomagnetic effects, it is easier to convert them into conductivities.

Components of the conductivity tensor can be expressed in terms of electron and hole mobilities, carrier concentration, tilt angle, and factors arising from the energy dependence of the relaxation time τ, i.e., the Hall and magnetoresistance factors A and M defined by the following equations:

$$A=\frac{\langle\tau^2\rangle}{\langle\tau\rangle^2},$$

$$M=\frac{\langle\tau^3\rangle}{\langle\tau\rangle^3}, \tag{7}$$

where the angular brackets denote the relevant energy averaging. Equations for partial conductivities of L electrons and T holes are given in Ref. 16.

Usually, carrier mobilities and densities of L electrons and T holes in bismuth are obtained by a least-squares fit of the measured resistivity components to their expression, assuming both Hall and magnetoresistance factors of electrons and holes to be close to unity.[6–10] This assumption is, however, not valid for electrons in bismuth[11,12] and Bi-rich Bi-Sb alloys[16] in the temperature range 100–300 K, where there is no strong statistical degeneracy.

The introduction of Hall and magnetoresistance coefficients in the usual least-squares method increases significantly the number of adjustable parameters (two per type of carrier), so that the accuracy of A and M is questionable. However, if we make some plausible assumptions concerning the relaxation time τ of charge carriers, we can calculate not only the A and M factors, but also all the transport coefficients by using a relatively small number of adjustable parameters. This approach gave excellent agreement between theoretical and experimental results in bismuth.[12] It will be extended to the alloy in the present work.

In a semimetal or an intrinsic semiconductor, the thermopower α_{ii} in the i direction is given by

$$\alpha_{ii}=\sum_j\left(\frac{\sigma_{ii}^j\alpha_j}{\Sigma_j\sigma_{ii}^j}\right), \tag{8}$$

where α_j are the partial thermopower of charge carriers j which are isotropic in most cases and σ_{ii}^j are the partial conductivities which may be anisotropic. In the set of axes (1,2,3), the tensor of the thermopower $\bar{\bar{\alpha}}$ of BiSb alloys is diagonal and has only two independent components $\alpha_{11}=\alpha_{22}$ and α_{33}.

Theoretical expressions of the conductivity tensor components and of the partial thermopower are given elsewhere.[15,16]

C. Scattering model and calculation procedure

As earlier,[11,12,16] we assume that there are two kinds of carrier scattering in bismuth-rich alloys, as in pure bismuth. Both scattering mechanisms are assumed to be elastic. The reciprocal relaxation time for L-electron scattering is given by[11]

$$\tau^{-1}(\varepsilon)=C_N\left(\frac{k_0T}{1\ \text{meV}}\right)^{3/2}\left\{\left(\frac{m_{dL}^*}{m_0}\right)^{3/2}\left[\varepsilon\left(1+\frac{\varepsilon}{\varepsilon_g}\right)\right]^{1/2}\times\left(1+2\frac{\varepsilon}{\varepsilon_g}\right)+x\left(\frac{m_{dT}^*}{m_0}\right)^{3/2}(\varepsilon_{LT}-\varepsilon)^{1/2}\right\},\quad(9)$$

where m_{dL}^* and m_{dT}^* are the density of states effective masses for one ellipsoid in the L and T bands, and ε, ε_g, and ε_{LT} the electron energy, the energy gap, and the energy overlap, respectively, in units of k_0T.

The first type of scattering in Eq. (9) is proportional to the density of states of the conduction L band and to the intraband constant C_N. This contribution includes the scattering of electrons by acoustical phonons, with the addition of the nonpolar scattering by optical phonons and of intervalley transitions within the conduction band. Moreover, scattering by the short-range potential of antimony atoms is possible in $Bi_{1-x}Sb_x$ alloys, with an energy dependence of the partial relaxation time like that for acoustical scattering. For scattering by acoustical phonons, the parameter C_N is multiplied by a factor which depends weakly on the temperature [Eq. (9)]. This dependence can change (increase or decrease with temperature) due to the other above-mentioned mechanisms of scattering.

The second contribution in Eq. (9) concerns recombination scattering, i.e., electron transitions to the valence T band. The corresponding reciprocal relaxation time is proportional to the density of states of the T band and to the recombination constant C_R. A dimensionless parameter $x=C_R/C_N$ was used instead of C_R.

Since the light L-hole band and the L-electron band are mirrorlike bands, the same expression as Eq. (9) is also valid for L holes without any new scattering parameters. The model of the T-hole relaxation process is also similar to that described above.[11] It involves a constant C_P that is analogous to C_N and represents the intensity of hole scattering by accoustic phonons. The recombinational scattering of holes is governed by the same parameter C_R (or x) as for L electrons.

Although the density of states of light L holes is lower than that of T holes, we included their contribution in the program of calculation. Generally, this contribution was neglected in all studies performed on Bi.[6–12]

The three scattering parameters C_N, C_P, and x were adjusted at each fixed temperature by a least-squares procedure. The overlap of the conduction L band with the valence T band, E_{LT}, was another adjustable parameter. We also selected the tilt angle θ between the principal axis of the electron ellipsoid and bisextric axis. However, this angle turned out to be relatively insensitive to temperature and was found close to 7°.

The adjustable parameters of the model were obtained by a least-squares fit of experimental coefficients to their theoretical expressions calculated by numerical integration. As in Ref. 12, but in contrast with Refs. 6–11, we used simultaneously 12 galvanomagnetic coefficients and 2 thermopower components.

Using the initial and adjustable band and scattering parameters, we calculated the electron reduced chemical potential ζ^*, the carrier densities, the components of mobilities in the principal axes of the ellipsoids, the Hall factor A, the magnetoresistance factor M, and the partial thermopowers of the three types of carriers: L electrons, T holes, and L holes. The reduced chemical potential was calculated from the condition of electrical neutrality, namely,

$$N=P+p,\quad(10)$$

where N, P, and p are the densities of L electrons, T holes, and L holes, respectively.

III. EXPERIMENT

A. Samples

A homogeneous ingot of $Bi_{0.96}Sb_{0.04}$ was prepared by the traveling heater method.[24] To be brief, this technique consists in moving a liquidus composition through material of the corresponding solidus composition by lowering an ampoule into a furnace. High-purity (99.999%) bismuth and antimony were used as starting materials. Care was exercised during growth to eliminate constitutional supercooling effects by using a slow growth rate (8 mm/day) with a temperature gradient estimated at 35 °C/cm. The grown ingot was 15 cm in length and 15 mm in diameter. After about 2 cm, the grown ingot was composed almost entirely of one single grain.

The compositional homogeneity was checked by the electron beam microprobe technique. There was about a 10% variation in the mean antimony content along the length of the ingot, which is quite remarkable. The radial inhomogeneity is less than 3% of the mean composition.[16]

Samples used for various measurements (Table II) were cut along the desired crystallographic directions in homogeneous single-crystalline portions of the ingot, which had been oriented by the x-ray back reflection Laue method from (111) primary cleavage planes. The four samples used had parallelepipedic shape and their approximate dimensions are reported in Table II. It was found preferable to measure the R_{123} coefficient separately on a thin sample, because this coefficient is nearly one order of magnitude smaller than R_{231}. The edges of samples 1, 2, and 4 were parallel to the main crystallographic axis, while sample 3 had its axis in the (1,2) plane inclined at an angle of 15° with respect to the 1 direction.

One end of samples 1, 2, and 4 was soldered with Wood alloy on a copper plate electrically insulated from a vertical cryostat which has been described in detail elsewhere.[16,25] The essential feature of this cryostat is that it was designed to ensure strict isothermal conditions on the sample. The main problem with the $Bi_{0.96}Sb_{0.04}$ alloy is that the two components of the thermopower are relatively high ($\alpha_{33}\approx -100\ \mu$V/K and $\alpha_{11}\approx -65\ \mu$V/K in the investigated temperature range), leading to an additional contribution to the Ohmic voltage, due to the Peltier effect, when a direct current flows across the sample. This voltage may still be enhanced by the application of a magnetic field if the temperature gradient remains due to thermomagnetic effects. In order to reduce this gradient, the cold end of the sample was heated with a small electrical resistor.

The two components of the thermopower were measured by the conventional method with samples 1 and 2.

TABLE II. Summary of experimental conditions (approximate sample dimensions, direction of current, magnetic field, and measured emf) used to obtain the magnetoresistivity coefficients. 1, 2, and 3 are related to the binary, bisectrix, and trigonal axes, respectively.

Sample number	Dimension (mm)[a]			Direction of			Measured coefficient
	a	*b*	*l*	*J*	*B*	*E*	
1	2.3	2.4	12.5	3		3	ρ_{33}
1	[1]	[2]	[3]	3	1	3	A_{31}
1				3	3	3	A_{33}
1				3	2	1	R_{231}
2	2	1.4	14	1		1	ρ_{11}
2	[2]	[3]	[1]	1	1	1	A_{11}
2				1	2	1	A_{12}
2				1	3	1	A_{13}
2				1	2.3 plane	1	A_{14}
3	2.3	1.5	14.4	1.2 plane	J.3 plane	3	A_{41}
3	[3]	[1.2] plane	[1.2] plane	1.2 plane	J.3 plane	3	A_{44}
4	3.3	0.42	14.7	1	3	2	R_{123}
	[2]	[3]	[1]				

[a]The direction 1, 2, or 3 is indicated in brackets.

B. Experimental procedure

The precise orientation of the sample placed in the cryostat was checked with the help of the variations of the magnetoresistance with the magnetic field direction.[16] The resistivity under zero magnetic field was obtained from an average of more than five independent measurements, each being carried out with two directions of the current. For each measurement, the voltage was read almost instantaneously. Then, taking residual effects into account, the resistivity was measured as a function of magnetic field, oriented in order to determine the desired coefficient. The intensity of the magnetic field was varied, and linear variations of the magnetoresistance with B^2 were observed up to around 50–400 G, depending on the crystallographic direction and the temperature. An example of magnetoresistance is shown in Fig. 2 at 78 K, where the low-field limit is around 200 G. Typical magnetoresistance values, less than 10% at 78 K and 1% at 300 K, were observed, requiring a resolution of 10^{-8} V in emf measurements for a sample current of 0.4 A.

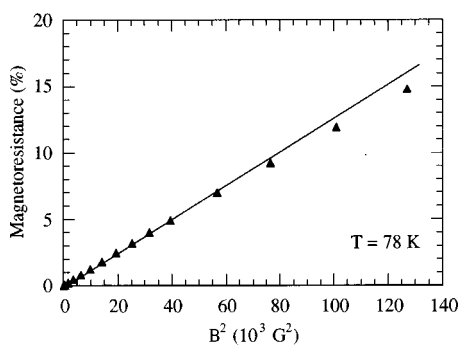

FIG. 2. Magnetoresistance in the binary direction of sample No. 2 (Table II) as a function of magnetic field B parallel to the trigonal axis for $T=78$ K. The low-field condition (solid line) is observed up to a value of 200 G. The slope at low fields gives A_{13}.

Hall effect measurements require in principle only two contacts perpendicular to the current. In practice, the two contacts cannot be exactly put in line on the sample and the resulting measured voltage includes a longitudinal contribution. We used three contacts as shown in Fig. 3(b). The measured voltages V_1 and V_2 under a magnetic field satisfy the relations

$$V_1 = V_1^H + \alpha V,$$

$$V_2 = V_2^H + (\alpha - 1)V, \tag{11}$$

where, referring to Fig. 3, V_1^H and V_2^H are the Hall voltages, V the longitudinal voltage, and α a geometrical factor determined by measurements without a magnetic field. The Hall voltage is then given by the average value of V_1^H and V_2^H.

We performed measurements at seven temperatures between 77 and 300 K.

IV. RESULTS AND DISCUSSION

A. Experimental results

The temperature dependences of the low-field galvanomagnetic coefficients in the $Bi_{0.96}Sb_{0.04}$ alloy are shown in Fig. 3. The two zero-field isothermal resistivities ρ_{11} and ρ_{33} follow a linear law in the studied temperature range as in pure bismuth[10] [Fig. 3(a)]. This metallic behavior is, however, purely fortuitous and is due to the combined effects of the peculiar carrier-scattering mechanisms and of the temperature dependence of both effective masses and carrier densities. This will be discussed later.

One order of magnitude separates the two Hall coefficients $-R_{123}$ and R_{231}, which both follow a $T^{-1.8}$ law [Fig. 3(b)]. The main term R_{231} is slightly greater than for pure bismuth.[10]

The variations versus temperature of all the A_{ij} coefficients follow nearly a $T^{-4.5}$ law above 120–140 K, but be-

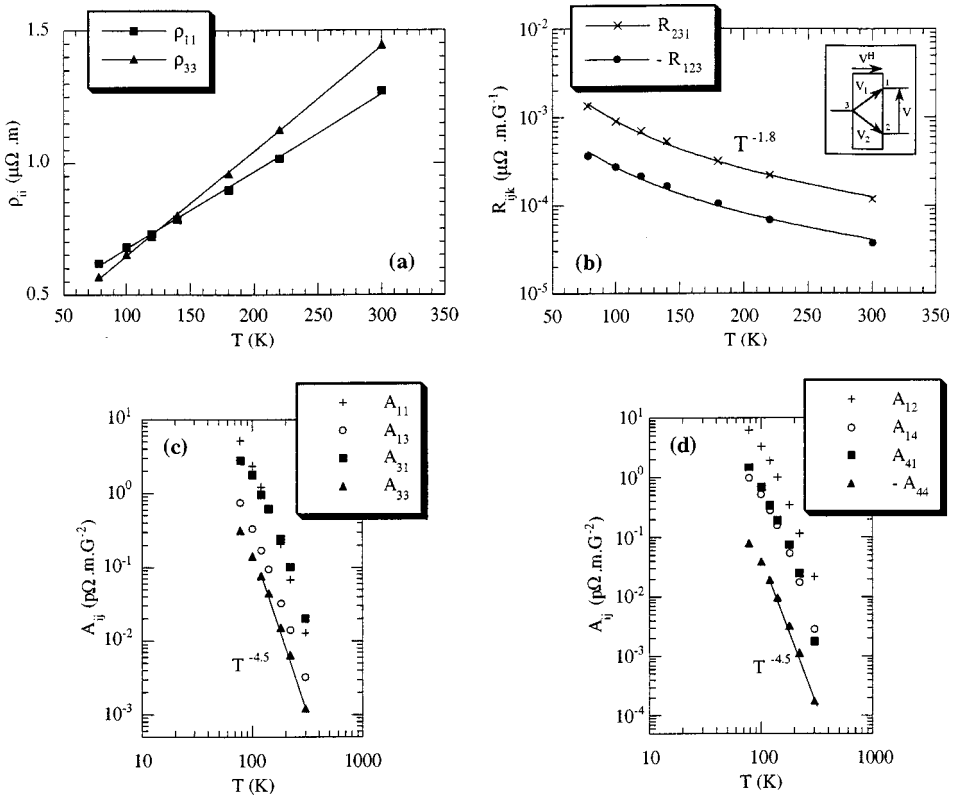

FIG. 3. Low-field galvanomagnetic coefficients as a function of temperature in the $Bi_{0.96}Sb_{0.04}$ alloy. (a) Isothermal resistivities ρ_{11} and ρ_{33}. (b) Hall coefficients R_{231} and $-R_{123}$. The arrangement of Hall voltage contacts is drawn in the inset. The measured voltage V_1 or V_2 is related to the Hall voltage V^H and the longitudinal voltage V. (c) A_{11}, A_{13}, A_{31}, and A_{33} coefficients. (d) A_{12}, A_{14}, A_{41}, and $-A_{44}$ coefficients.

low this temperature the variations seem to be weaker [Figs. 3(c) and 3(d)]. The slope change appears at a temperature near the Debye temperature θ_D. In pure bismuth, similar observations were made by Michenaud and Issi.[10] However, the breaking near $\theta_D = 120$ K was more abrupt with the passage from a T^{-2} law (for $T < \theta_D$) to a $T^{-3.9}$ variation.

Some scarce results on magnetoresistance coefficients were given in the literature[26,27] for two close $Bi_{1-x}Sb_x$ compositions $x = 0.03$ and $x = 0.05$ at a fixed temperature near 80 K. The reported values are in good agreement with our results, except for the large Hall factor R_{231}, which presents higher values than those obtained in this study.

The variations with temperature of the thermoelectric power are reported elsewhere.[16]

B. Calculated parameters of the model, mobilities, and concentrations

Following the procedure described above in Sec. II C and using the band parameters of Sec. II A, the adjustable parameters of the model were calculated as a function of temperature. The values are reported in Table III.

All initial parameters depend on the temperature like those of pure bismuth.[12] The overlap E_{LT} in the alloy is less than in Bi, in agreement with the known band model (see Fig. 1). However, it increases with temperature more quickly.

With the set of initial parameter values, we calculated the relative chemical potential of electrons, the carrier densities, the mobilities, the Hall and magnetoresistance factors, and the partial thermopowers of L electrons, L holes, and T holes (Table IV and Fig. 4).

The contribution of the light L holes to transport coefficients turned out to be very small in comparison with that of L electrons and T holes. For example, the partial conductivity of L holes is three orders of magnitude less than that of electrons at 77 K and one order at 300 K. Therefore, their contribution can be neglected. The physical reason is their very small density due to the low position of the L maximum in comparison to the T maximum of the valence band. On the other hand, we found that the mobility of electrons along the major axis of the ellipsoid, $\mu_{2'}$, is two orders of magnitude smaller than $\mu_{1'}$ and $\mu_{3'}$ in the investigated tempera-

TABLE III. Initial parameter values used in the calculation of the transport coefficients.

T (K)	C_N (10^{11}/s)	C_P (10^{11}/s)	x	E_{LT} (meV)
78	6.27	4.53	0.29	36
100	5.26	6.00	0.28	43
120	4.72	8.48	0.26	51
140	4.25	9.31	0.29	58
180	3.47	11.6	0.34	76
220	2.78	15.0	0.42	98
300	1.67	27.0	0.58	148

TABLE IV. Calculated transport coefficients as a function of temperature in the $Bi_{0.96}Sb_{0.04}$ alloy: the electron reduced chemical potential ζ^*, the Hall and magnetoresistance factors A_N, M_N, A_P, and M_P, and the partial thermopowers α_N and α_P of L electrons and T holes, respectively.

T (K)	ζ^*	A_N	M_N	A_P	M_P	α_N (μV/K)	α_P (μV/K)
78	4.2	1.19	1.62	1.04	1.12	−95	152
100	3.6	1.25	2.14	1.04	1.14	−95	142
120	3.3	1.45	2.99	1.05	1.15	−92	130
140	3.0	1.54	3.55	1.04	1.13	−94	123
180	2.5	1.73	4.96	1.03	1.1	−97	108
220	2.2	1.93	6.65	1.02	1.07	−102	94
300	1.4	2.47	12.1	1.01	1.04	−116	70

ture range and the mobility of T holes along the trigonal axis, ν_3, one order of magnitude smaller than ν_1.

The temperature dependences of mobilities and of the carrier density ($N \approx P$) are shown in Fig. 4. We also included in the figure those obtained with bismuth.[12,28] It can be seen that the main effect of alloying is to reduce the mobility of T holes. Such a result confirms the observations made by Lenoir *et al.*[4] who investigated the anisotropy of the thermopower. The temperature behaviors of the carrier density in the alloy and in Bi from 4.2 to 300 K are quite similar to one another, the metallic behavior being, however, more pronounced in bismuth than in the alloy due to the larger overlap at low temperature. At 4.2 K, we took the value of 2×10^{22} m^{-3}, determined by Brandt *et al.*[22] for a close composition ($x=0.046$).

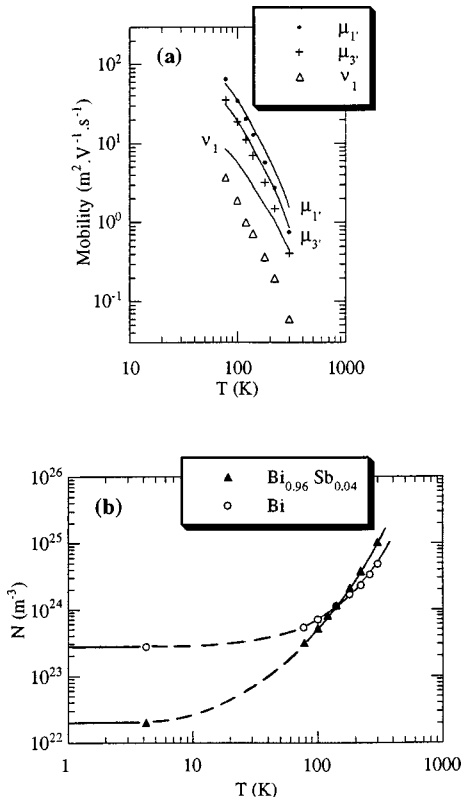

FIG. 4. Transport coefficients in the $Bi_{0.96}Sb_{0.04}$ alloy. (a) Temperature dependences of L-electron ($\mu_{1'}$ and $\mu_{3'}$) and T-hole (ν_1) mobilities. Comparison with bismuth (Ref. 12) (solid lines). (b) Temperature dependence of the carrier density in the alloy and in bismuth after Ravich *et al.* (Ref. 12). Points at 4.2 K were obtained by Brandt *et al.* (Ref. 22) in the $Bi_{0.954}Sb_{0.046}$ alloy and by Bhargava (Ref. 28) in Bi.

The electron factors A_N and M_N rise with temperature and are much larger than unity, whereas the corresponding factors for T holes, A_P and M_P, are close to unity (Table IV). The deviation from unity for electrons is more pronounced than in bismuth.[12] For example, at $T=300$ K, $A_N=1.68$ and $M_N=4.11$ in Bi. It is due to the lower reduced chemical potential ζ^* and to the larger nonparabolicity of electrons.

Deviation from unity of both factors A_N and M_N can be confirmed directly through an analysis of the galvanomagnetic coefficients. Taking into account that the two small mobilities $\mu_{2'}$ and ν_3 as well as the tilt angle can be neglected in bismuth, several useful simplified expressions can be derived[7,12,16] from the set of galvanomagnetic coefficients, including the approximate formula[29]

$$A_{12}-A_{11}\approx 2A_{11}\left(1-\frac{A_N^2}{M_N}\right). \tag{12}$$

Since this expression holds in the alloy, we can compare the theoretical calculated factor A_N^2/M_N to that derived from experimental magnetoresistance coefficients applying Eq. (12). The theoretical and experimental curves of A_N^2/M_N versus temperature are represented in Fig. 5. We can see that the two curves are close to each other.

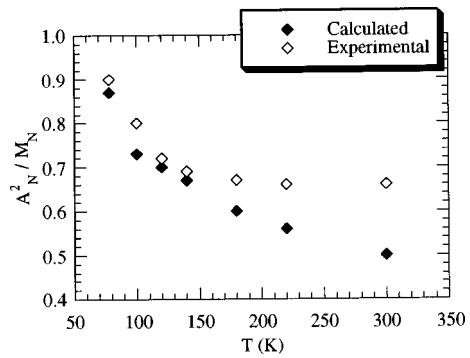

FIG. 5. Comparison of the temperature dependence of the factor A_N^2/M_N calculated and obtained directly from the two experimental magnetoresistance components A_{11} and A_{12} according to Eq. (12).

The considerable difference between A_{11} and A_{12} and its increase with temperature represent a direct experimental proof that A_N and M_N factors differ from unity in the expression for the galvanomagnetic coefficients. Another qualitative proof can be obtained through the calculation of the large magnetoresistance coefficient A_{31}. With the same approximations as in Eq. (12), the expression for A_{31} can be obtained[16] as follows:

$$A_{31} \approx \frac{1}{eN}\left[M_N \nu_1 + (M_N - A_N^2)\,\frac{\mu_{1'}}{2}\right]\left[1+\frac{2\nu_1}{\mu_{1'}}\right]^{-1}. \quad (13)$$

If the factors A_N and M_N are equal to 1, only the relatively small hole mobility ν_1 would contribute to A_{31}. Such a calculated value of A_{31} would then be several times lower than the experimental one. If nonunit factors are used, the second item in Eq. (13) is greater than the first one, and the calculated A_{31} value is found to be close to the measured one. If we try to increase the hole mobility in order to calculate the good coefficient A_{31} without the second item, we would obtain a large difference between the two components of the thermopower, in disagreement with experimental data.

It should be noted that the proof that the factors A_N and M_N deviate substantially from unity is totally independent of any assumptions regarding the scattering mechanisms or band nonparabolicity. The proof relies exclusively on experimental data and the existing qualitative argument regarding a multiellipsoid structure of the conduction band in the $Bi_{0.96}Sb_{0.04}$ alloy.

V. CONCLUSION

The complete set of the 12 galvanomagnetic coefficients was measured for the $Bi_{0.96}Sb_{0.04}$ alloy in the 77–300 K temperature range in weak magnetic fields. As previously considered for bismuth,[12] a theoretical model was developed based on some assumptions on the carrier-scattering mechanisms. The adjustable parameters of the model were determined using a least-squares method between calculated and experimental values of the 12 galvanomagnetic coefficients and the two components of the thermopower. The obtained results showed that the scattering constants change in the alloy in comparison with pure Bi. These constants are expressed through matrix elements of the interaction of electrons with phonons and, thus, are determined by electron wave functions. In their turn, the wave functions at the L point of the Brillouin zone depend on energy distances between the edge of conduction band and other neighboring bands at the same point (besides the nearest band of light L holes determining the nonparabolicity). The other bands influence, in particular, spin-orbit mixing. The possible effect of these bands is not within the framework of the applied two-band approximation. Dependences of the energy distances and the wave functions as a function of composition x are unfortunately unknown at present. The second reason for the dependence of scattering constants on x is the scattering by the short-range potential of Sb atoms in the alloy. This mechanism of scattering gives the same energy dependence of relaxation time as the electron-phonon scattering. The scattering constants increase due to this effect just as a sign of the spin-orbit effect is not definite.

The carrier mobilities and densities are found to be near the values of pure bismuth, but the effect of alloying is more important for hole than for electron mobilities. Calculated values of the Hall and magnetoresistance factors of electrons show a substantial deviation from unity in the temperature range investigated. These values are greater than in pure bismuth, and they arise from the energy dependence of the relaxation time due to the large nonparabolicity of the L bands.

The extension of the study to other antimony contents, especially in the semiconducting range, which present a great interest from the point of view of thermoelectricity, is the next step for investigating the transport properties. Such investigations should undoubtedly contribute to a best comprehension of scattering mechanisms in these alloys.

ACKNOWLEDGMENTS

The authors would like to thank A. Dauscher and P. Carayon for helpful discussions. One of the authors (B.L.) is indebted to Professor J.-P. Issi and Professor J.-P. Michenaud for initiating this work. The investigation was supported by the program ''Integration,'' project number 75.

[1] A. L. Jain, Phys. Rev. **114**, 1518 (1959).
[2] G. E. Smith and R. Wolfe, J. Appl. Phys. **33**, 841 (1962).
[3] W. M. Yim and A. Amith, Solid-State Electron. **15**, 1141 (1972).
[4] B. Lenoir, M. Cassart, J.-P. Michenaud, H. Scherrer, and S. Scherrer, J. Phys. Chem. Solids **57**, 89 (1996).
[5] B. Lenoir, A. Dauscher, M. Cassart, H. Scherrer, and Yu. Ravich, J. Phys. Chem. Solids **59**, 129 (1998).
[6] R. N. Zitter, Phys. Rev. **127**, 1471 (1962).
[7] R. Hartman, Phys. Rev. **181**, 1070 (1969).
[8] B. Abeles and S. Meiboom, Phys. Rev. **101**, 544 (1956).
[9] J. Okada, J. Phys. Soc. Jpn. **12**, 1327 (1957).
[10] J.-P. Michenaud and J.-P. Issi, J. Phys. C **5**, 3061 (1972).
[11] Yu. I. Ravich and A. V. Rapoport, Sov. Phys. Solid State **34**, 960 (1992).
[12] Yu. I. Ravich, Yu. V. Ivanov, and A. V. Rapoport, Semiconductors **29**, 458 (1995).
[13] E. E. Mendez, Ph.D. thesis, MIT, Boston, 1979.
[14] M. P. Vecchi and M. S. Dresselhaus, Phys. Rev. B **10**, 771 (1974).
[15] V. A. Nemchinsky and Yu. I. Ravich, Sov. Phys. Solid State **33**, 1165 (1991).
[16] A. Demouge, B. Lenoir, Yu. I. Ravich, H. Scherrer, and S. Scherrer, J. Phys. Chem. Solids **56**, 1155 (1995).
[17] E. J. Tichovolsky and J. G. Mavroides, Solid State Commun. **7**, 927 (1969).
[18] G. Oelgart and R. Herrmann, Phys. Status Solidi B **75**, 189 (1976).
[19] Y. H. Kao, Phys. Rev. **129**, 1122 (1963).

[20] B. Lax and J. G. Mavroides, in *Advances in Solid State Physics*, edited by F. Seitz and D. Turnbull (Academic, New York, 1960), Vol. 11, p. 261.

[21] E. E. Mendez, A. Misu, and M. S. Dresselhaus, Phys. Rev. B **24**, 639 (1981).

[22] N. B. Brandt, Kh. Dittmann, and Ya. G. Ponomarev, Sov. Phys. Solid State **13**, 2408 (1972).

[23] E. A. Dorofeev and L. A. Fal'kovskii, Sov. Phys. JETP **60**, 1273 (1984).

[24] B. Lenoir, M. Cassart, A. Demouge, J. P. Michenaud, D. Perrin, H. Scherrer, and S. Scherrer, J. Phys. Chem. Solids **56**, 99 (1995).

[25] J.-P. Issi, J.-P. Michenaud, A. Moureau, and P. Coopmans, J. Phys. E **4**, 512 (1971).

[26] T. Yazaki and Y. Abe, J. Phys. Soc. Jpn. **24**, 290 (1968).

[27] C. B. Thomas and H. J. Goldsmid, J. Phys. C **3**, 696 (1970).

[28] R. N. Bhargava, Phys. Rev. **156**, 785 (1967).

[29] The formula $A_{12} \approx A_{11}$, represented without any application in our previous article (Ref. 16), is valid provided $A = M = 1$ only.